The Zn^{2+}-sensing receptor, ZnR/GPR39, upregulates colonocytic Cl^- absorption, via basolateral KCC1, and reduces fluid loss[*]

Laxmi Sunuwar[a], **Hila Asraf**[a], **Mark Donowitz**[b], **Israel Sekler**[a], and **Michal Hershfinkel**[a,*]

[a]Department of Physiology and Cell Biology, Faculty of Health Sciences, Ben-Gurion University of the Negev, Beer Sheva, Israel

[b]Department of Medicine, Division of Gastroenterology, Johns Hopkins University School of Medicine, Baltimore, MD 21205, USA

Abstract

Administration of zinc, as a complement to oral rehydration solutions, effectively diminishes duration and severity of diarrhea, but it is not known whether it merely fulfills a nutritional deficiency, or if zinc has a direct role of regulating solute absorption. We show that Zn^{2+} acts via a specific receptor, ZnR/GPR39, to reduce fluid loss. Intestinal fluid secretion triggered by cholera toxin (CTx) was lower in WT mice compared to ZnR/GPR39 KO. In the absence of dietary Zn^{2+} we observed similar fluid accumulation in WT and ZnR/GPR39 KO mice, indicating that Zn^{2+} and ZnR/GPR39 are both required for a beneficial effect of Zn^{2+} in diarrhea. In primary colonocytes and in Caco-2 colonocytic cells, activation of ZnR/GPR39 enhanced Cl^- transport, a critical factor in diarrhea, by upregulating K^+/Cl^- cotransporter (KCC1) activity. Importantly, we show basolateral expression of KCC1 in mouse and human colonocytes, thus identifying a novel Cl^- absorption pathway. Finally, inhibition of KCC-dependent Cl^- transport enhanced CTx-induced fluid loss. Altogether, our data indicate that Zn^{2+} acting via ZnR/GPR39 has a direct role in controlling Cl^- absorption via upregulation of basolateral KCC1 in the colon. Moreover, colonocytic ZnR/GPR39 and KCC1 reduce water loss during diarrhea and may therefore serve as effective drug targets.

Keywords

Zinc signaling; Zinc sensing receptor; ZnR/GPR39; Diarrhea; K^+/Cl^- cotransporter; KCC

---

1. Introduction

Despite the profound effect that oral rehydration therapy (ORS) has made on diarrhea treatment, diarrhea still remains a leading cause of morbidity and mortality in many parts of the world [1,2]. Some diarrheal diseases result from impaired activity of ion transporters in colonic epithelial cells (colonocytes) that leads to excessive water secretion [3]. Coordinated activity of apical and basolateral ion transporters in colonocytes is essential for conserving Na^+, K^+ and Cl^- and for maintaining electrochemical and pH equilibrium of the cells [4]. Among the most common causes of diarrhea is infection by *V. cholera*. Cholera toxin (CTx) enhances production of cAMP, thereby up-regulating the activity of the cystic fibrosis transmembrane conductance regulator (CFTR), and enhancing intestinal Cl^- efflux. In addition, CTx also inhibits the activity of Na^+/H^+ exchanger 3, which decreases Na^+ absorption. Taken together, the ionic imbalance that results from loss of Cl^- and Na^+ produces the driving force for water loss, the hallmark of diarrhea. Possible strategies for reducing the Cl^- efflux into the lumen involve blocking apical CFTR or Ca^{2+} activated Cl^- channels [5]. The nuclear bile acid receptor FXR has been shown to downregulate Cl^- secretion and is suggested as a target for antidiarrheal drugs [6]. Surprisingly, mechanisms mediating Cl^- movement across the basolateral membrane, to support Cl^- absorption, are still not fully identified [4,7].

Diarrhea is commonly associated with insufficient dietary zinc (Zn^{2+}) intake, particularly in children, a situation that may be amplified by loss of Zn^{2+} as consequence of the disease itself [8]. Treatment with Zn^{2+} supplemented oral rehydration solutions (ORS) substantially attenuates duration and severity in cases of both acute and persistent diarrhea [9,10] and often is effective even under Zn^{2+} sufficient diet [11, 12]. Although the underlying mechanism in unknown, the World Health Organization (WHO) and United Nations Children's Fund (UNICEF) have recommended Zn^{2+} supplementation as a therapeutic agent for treating acute diarrhea [12,13]. Previous studies have suggested that Zn^{2+} affects Cl^- secretion via regulation of cAMP, Ca^{2+} or Na^+ dependent pathways [9,12,14–18], but how Zn^{2+} interacts with these pathways is not well understood. Hence, it is important to determine if Zn^{2+} supplementation is important for the recovery of this essential dietary micronutrient, or if Zn^{2+} has a direct therapeutic target that can regulate solute absorption in the colon.

We have functionally identified a Zn^{2+}-sensing receptor that mediates Zn^{2+}-dependent signaling in epithelial cells; and termed it ZnR [19–21]. Later studies based on ectopic expression systems or tissues from genetically knockout mice [22–25] have firmly linked ZnR activity to the orphan protein GPR39 [22–25]. Moreover, Zn^{2+} was identified as the ligand of GPR39 [26–28], and not obestatin that was initially associated with this receptor [29–31]. The ZnR/GPR39 is activated by extracellular Zn^{2+} at the concentration range physiologically found in the digestive tract. Colon epithelial cells exhibit ZnR/GPR39 activity [20], which controls colonocytes growth and differentiation [20,32–34]. In colonocytes, extracellular Zn^{2+} induces ZnR/GPR39 activation that triggers a Gq dependent metabotropic release of Ca^{2+} [19,26], and subsequent activation of the mitogen activated protein kinase (MAPK), extracellular regulated ERK1/2, pathway [19]. The ZnR/GPR39 signaling pathway subsequently upregulates Na^+/H^+ exchange activity [20,32], thereby

promoting recovery from acidic pH_i [5,35,36]. In neurons, ZnR/GPR39 activity was also shown to upregulate K^+/Cl^- cotransport activity, KCC2, and thereby Cl^- transport. Although both Zn^{2+} and Cl^- have important roles in diarrhea, it is unknown if they are linked. We therefore sought to determine if the colonocytic ZnR/GPR39 mediates the therapeutic effects of Zn^{2+} by regulating Cl^- transport.

2. Results

2.1. ZnR/GPR39 expression reduces cholera toxin (CTx) induced fluid accumulation

Excessive fluid loss is a hallmark of diarrheal diseases, we therefore asked whether ZnR/GPR39 regulates fluid accumulation. Under control conditions, the weight of intestinal fluid in both WT and ZnR/GPR39 KO mice was not detectable. We then treated WT and ZnR/GPR39 KO mice with cholera toxin (20 μg CTx, Fig. 1A) that triggers fluid secretion. After 6 h, the accumulated intestinal fluid was weighed and normalized to initial body weight. Treatment with CTx increased intestinal fluid in WT mice (0.025 ± 0.003 mg/kg body weight, Fig. 1B high-Zn^{2+} diet) compared to that in untreated controls. A further significant increase in intestinal fluid was measured in CTx-treated ZnR/GPR39 KO mice (0.035 ± 0.003 mg/kg body weight, Fig. 1B high-Zn^{2+} diet) compared to WT mice, suggesting a protective effect of ZnR/GPR39 that reduces CTx-induced fluid secretion.

If Zn^{2+} is required for ZnR/GPR39 activation, then a Zn^{2+} deficient diet would be expected to negate the differences between WT and ZnR/GPR39 KO animals. We therefore compared fluid accumulation following a short (4-week) exposure to a moderate Zn^{2+}-deficient diet or a severe Zn^{2+}-deficient diet [37]. No changes in food intake, animal behavior or skin/hair were observed in mice fed moderate Zn^{2+} diet or Zn^{2+}-deficient diet. Intestinal fluid volume was then monitored following 6 h of CTx treatment (as above). The results indicate that in WT mice, receiving moderate-Zn^{2+} diet, CTx induced less secretion (0.038 ± 0.003 mg/kg body weight, Fig. 1B moderate-Zn^{2+}) compared to ZnR/GPR39 KO mice (0.048 ± 0.002 mg/kg body weight, Fig. 1B moderate-Zn^{2+}). Our results further show that 4-week treatment with a moderate-Zn^{2+} deficient diet were already sufficient to trigger significantly increased fluid accumulation, in WT and ZnR/GPR39 KO mice, compared to the fluid levels observed in mice that received the high-Zn^{2+} diet. Nevertheless, ZnR/GPR39 similarly protected the animals from diarrhea under both high and moderate Zn^{2+} levels (Fig. 1C). In contrast, when mice were subject to 4-weeks of severe Zn^{2+}-deficient diet, the volume of accumulated fluid in WT or ZnR/GPR39 KO mice were not significantly different (0.041 ± 0.002 mg/kg body weight in WT versus 0.043 ± 0.002 mg/kg body weight in ZnR/GPR39 KO; Fig. 1B Zn^{2+}-deficient). This suggests that in the absence of Zn^{2+}, ZnR/GPR39 cannot reduce fluid accumulation. Accumulated fluid volume in mice fed severe Zn^{2+}-deficient diet did not significantly increase compared to that in the mice fed a moderate-Zn^{2+} diet. This may be explained by an adaptive response to the switch from normal to low Zn^{2+} level. Such adaptive response to dietary Zn^{2+} deficiency was shown in ZnT3 KO mice [38] and may be affected by diet-dependent regulation of the ZIP transporters [39–41]. Extracellular Zn^{2+} changes may also modulate ZnR/GPR39 activity via its desensitization or resensitization [20,21]. Notably, comparison of fluid accumulation between WT and ZnR/GPR39 KO mice (Fig. 1C) shows that in the presence of sufficient dietary Zn^{2+} (high-Zn^{2+} or moderate Zn^{2+}

diets) ZnR/GPR39 KO have much larger fluid accumulation than WT, while in the severe Zn^{2+} deficiency this is abolished. Considering the well-established effects of dietary Zn^{2+} in diarrhea, this experiment suggests that protection from CTx-induced fluid secretion is dependent on Zn^{2+} activation of ZnR/GPR39.

2.2. ZnR/GPR39 upregulates K^+-dependent Cl^- transport in colonocytes

We next asked how ZnR/GPR39 affects fluid secretion. We initially used undifferentiated Caco-2 colonocytes that exhibit Zn^{2+}-dependent signaling mediated by ZnR/GPR39 via a Gq-dependent pathway (Fig. 2A, B), in agreement with previous studies [33,34]. Importantly, the paradigm that triggers Zn^{2+}-dependent ZnR/GPR39 signaling does not induce Zn^{2+} permeation into these cells (Fig. 2C). Since K^+-dependent Cl^- cotransporters (KCC and NKCC) are fundamental gatekeepers of Cl^- gradients, and thereby, of fluid movement across the colonic epithelium, we asked if they are regulated by Zn^{2+}. In order to test this, Caco-2 colonocytes were subjected to the well-established NH_4Cl paradigm [42] that determines K^+/Cl^- cotransport activity in cells loaded with the pH sensitive dye BCECF ([42–44], see also Section 4). Addition of NH_4Cl (10 mM) resulted in cellular alkalinization due to passive entry of NH_3 into the cells (Fig. 2D–E, [43]). This was followed by influx of NH_4^+ that serves as a surrogate for K^+ (see Section 4) and is likely transported into the cell by KCC/NKCC [42–44]. The initial rate of intra-cellular acidification likely represents NKCC/KCC-dependent Cl^- transport, as we and others demonstrated [42–44]. Extracellular pH is not altered using this paradigm and therefore the interaction of Zn^{2+} with ZnR/GPR39 is unlikely to be affected [24,45]. To study the effect of ZnR/GPR39 on Cl^- transport, Caco-2 cells were pre-treated with 100 μM Zn^{2+}, which activates ZnR/GPR39 without affecting intracellular Zn^{2+} [20]. The acidification rate, representing NKCC/KCC transport activity, was approximately 50% higher in cells pre-treated with Zn^{2+} compared to controls (Fig. 2D, E). To determine if the effect of Zn^{2+} is mediated by ZnR/GPR39-dependent signaling we inhibited the Gq path-way, which abolished the Zn^{2+}-dependent Ca^{2+} response (Fig. 2B). Addition of the Gq inhibitor, YM254890 (1 μM) reversed the effect of Zn^{2+} on ion transport. Since phosphorylation activated by ZnR/GPR39 may affect NKCC/KCC dependent transport [44], we also inhibited ZnR/ GPR39-dependent ERK1/2 activation [20] while monitoring ion transport using the BCECF paradigm. The Zn^{2+}-dependent upregulation of cotransport activity was completely reversed by the MAPK inhibitor U0126 (1 μM) (Fig. 2D, E). Since activation of the Gq-dependent Ca^{2+} response and ERK1/2 by Zn^{2+} are largely mediated by ZnR/GPR39 in colonocytes [20,33], this experiment suggests that ZnR/GPR39 signaling is required for upregulation of ion transport.

The K^+-dependent Cl^- transporters require Cl^- to mediate ion transport, we therefore asked if the ion transport monitored in the BCECF paradigm is Cl^- dependent. Cells loaded with BCECF were perfused with a Cl^--free solution (see Section 4) and 10 mM $(NH_4)2HPO_4$ was applied, resulting in alkalinization of the cytoplasm (Fig. 3A). In the absence of Cl^- however, NH_4^+ transport was not observed and the cytoplasmic pH did not acidify in the presence or absence of Zn^{2+}. Suggesting the despite the presence of the K^+ surrogate ion (NH_4^+) ion transport was not mediated in the absence of Cl^-. This result suggests further that a K^+/Cl^- transporter is regulated by Zn^{2+} via ZnR/GPR39. To distinguish between KCC

and NKCC activity, we repeated the NH_4Cl paradigm in the absence of extracellular Na^+, which is essential for NKCC-dependent transport but not for KCC-dependent transport [46]. Zn^{2+}-dependent upregulation of Cl^- transport was maintained in the presence of a Na^+-free solution (NMDG iso-osmotically substituting Na^+, Fig. 2D, E). Thus, while NKCC may be expressed in the cells the transport we observe is Na^+ independent and this argues against a role of NKCC or other Na^+-coupled transporters, such as the Na^+/K^+ ATPase. As another control, we applied a well-established pharmacological approach to distinguish between KCC and NKCC dependent transport. Cells were treated with the diuretic compound bumetanide, at concentrations (1 or 20 μM), which primarily affect NKCC activity [44,47] and then NH_4^+ transport rate was determined. The NKCC inhibitor failed to reverse the effect of Zn^{2+} (Fig. 3B, C), supporting the conclusion that Zn^{2+}-dependent upregulation of ion transport is not mediated by NKCC. In contrast, application of the KCC inhibitor DIOA (40 or 100 μM [48–50]) reversed the upregulation of ion transport triggered by Zn^{2+} (Fig. 3B, C). Altogether, these experiments suggest that ZnR/GPR39 is upregulating KCC-dependent Cl^- transport. Importantly, under physiological conditions KCC utilizes the K^+ gradient to mediate Cl^- efflux out of the cells [51], while the experimental paradigm used in this set of experiments reverses the transporter activity. Our results therefore suggest that under physiological conditions ZnR/GPR39 activation induces Cl^- extrusion from colonocytes.

To directly monitor changes in intracellular Cl^-, cells were loaded with MQAE and exposed to 20 mM KCl that is expected to reverse KCC-dependent transport and induce Cl^- influx resulting in quenching of fluorescence [44]. Similar to what we observed using the NH_4Cl paradigm, pre-treatment with Zn^{2+} significantly enhanced intracellular Cl^- accumulation compared to control (Fig. 3D – F). Furthermore, the KCC inhibitor DIOA (40 μM) completely attenuated the effect of Zn^{2+} on Cl^- accumulation (Fig. 3F) but the NKCC inhibitor bumetanide (1 μM) did not reverse the effect of Zn^{2+} on the initial rate of fluorescence change (Fig. 3E, F). Bumetanide seemed to slightly attenuated the rate of acidification at later times (about 130–150 s), however this was not a significant effect. Altogether, these results provide further support for a role for Zn^{2+} in upregulating KCC-dependent Cl^- efflux under physiological ion gradients, which will enhance Cl^- absorption if the transporter is basolateral.

Three isoforms, KCC1 (422 bp), KCC3 (615 bp) and KCC4 (783 bp), are expressed in Caco-2 cells (Fig. 4A), while the neuronal KCC2 [52] is not. We therefore applied a molecular approach and silenced the expression of KCC1, KCC3 and KCC4 in Caco-2 colonocytes (Fig. 4B), and measured ion transport using the NH_4Cl paradigm. Application of Zn^{2+} to cells transfected with siKCC1 did not upregulate NH_4^+ transport (Fig. 4C – D),even though the siKCC1 decreased KCC1 expression level by about 50% (Fig. 4D upper panel). This degree of KCC1 silencing strongly inhibited the Zn^{2+}-dependent upregulation of K^+/Cl^- transport, resulting in similar rate as basal activity. Thus, residual KCC1 expression following the siKCC1 silencing was insufficient for mediating detectable ion transport. In contrast, Zn^{2+}-dependent upregulation of transport was fully maintained in control cells treated with a scrambled siRNA (SCR, Fig. 4D – E) or in cells transfected with the siKCC3 or siKCC4 constructs (Fig. 4F). Note that a small basal fluorescence change is apparent and not abolished by the silencing of either KCC isoforms, or DIOA (see Fig. 3),

which may be unrelated to KCC activity. Altogether, these results suggest that Zn^{2+}, via activation of ZnR/GPR39 signaling, upregulates KCC1 activity, thereby enhancing Cl^- transport.

2.3. KCC1 is expressed on the basolateral membrane in colon tissues

Analysis of KCC1 expression level, normalized to the ubiquitously expressed Na^+/K^+ ATPase, was performed in native colonocytes using tissues from WT and ZnR/GPR39 KO mice (Fig. 5A). Note that previous studies have indicated that under baseline conditions the histological organization of colon tissue from WT and ZnR/GPR39 KO are similar [34]. Immunofluorescence levels of the labeled proteins were similar in WT and ZnR/GPR39 KO mice, indicating similar expression levels of KCC1 in WT and Zn/GPR39 KO tissues (Fig. 5B – C). KCC1 staining was absent when the first antibody was omitted (right panels) or when a pep-tide antigen was used (Supplementary Fig. 1 and Section 4). Analysis of the "Mandar" overlap coefficient of KCC1 and the basolateral Na^+/K^+ ATPase indicated that in WT (0.82 ± 0.01) and ZnR/GPR39 KO (0.80 ± 0.01) colonocytes KCC1 cotransporter is expressed basolaterally (Fig. 5D). Importantly, KCC1 exhibited similar basolateral distribution in human colonocytes (Fig. 5E), with a "Mandar" overlap coefficient of 0.75 ± 0.01. Thus, expression of KCC1 and Na^+/K^+ ATPase largely overlapped in mouse and human tissue, suggesting that KCC1 mediates basolateral Cl^- extrusion in colonocytes.

2.4. Colonocytic KCC1 activity is upregulated by Zn^{2+} via ZnR/GPR39

Finally, we specifically asked if ZnR/GPR39 is involved in Zn^{2+}-de-pendent activation of K^+/Cl^- cotransport activity using polarized primary colonocytes from WT or ZnR/GPR39 KO mice. We first asked whether endogenous Zn^{2+} levels were similar in WT and ZnR/GPR39 KO mice. Tissue samples from the distal colon were loaded with Zinpyr-1 [53–55] and fluorescent signals were monitored in the presence or absence (control) of the high-affinity cell permeable Zn^{2+} chelator, TPEN (20 μM). The Zn^{2+}-dependent fluorescence levels were similar in control tissues from WT or ZnR/GPR39 KO, and application of TPEN significantly attenuated the fluorescent signal, indicating that the signal is triggered by Zn^{2+}. The decrease in the signal following application of TPEN was similar in both genotypes (Fig. 6A – B), suggesting that Zn^{2+} levels in colonocytes are similar in WT and ZnR/GPR39 KO mice. Using a similar approach it was previously shown that levels of neuronal vesicular Zn^{2+} were not different in WT and ZnR/GPR39 KO tissue [55].

We then compared rates of KCC activity in native colon segments from WT and ZnR/GPR39 KO mice (Fig. 6C – E). The rate of NH_4^+ transport (acidification) was about 30% higher in WT tissue compared to that in ZnR/GPR39 KO (Fig. 6E), suggesting that ZnR/GPR39 is required for upregulation of K^+/Cl^- transport. This transport activity may be triggered by endogenous Zn^{2+} released from colonocytes that activates ZnR/GPR39 in WT tissue. To test the role of Zn^{2+}, colon samples were prepared in the presence of the non-permeable Zn^{2+} chelator EDTA (100 μM, see Fig. 2A). Note that because of its high affinity to Zn^{2+} (Kd of $\sim 10^{-16}$), as compared to Ca^{2+} (Kd of $\sim 10^{-10}$), the non-permeable EDTA does not significantly affect Ca^{2+} levels [56,57]. Addition of EDTA to the apical side of the tissue largely attenuated K^+/Cl^- transport in WT tissue (by about 25% of control tissues) bringing it to the level observed in ZnR/GPR39 KO tissues (Fig. 6C, E). This suggests that

endogenous Zn^{2+} is sufficient for inducing basal KCC activity in colonocytes. Attenuation of NH_4^+ transport was reversed when Zn^{2+} levels were recovered (by adding 200 μM in the presence of 100 μM EDTA) in WT tissue, thus restoring Zn^{2+}-dependent K^+/Cl^- transport activity (Fig. 6C, E). Significantly, EDTA treatment of ZnR/GPR39 KO tissues did not alter the rate of transport (Fig. 6D – E). Thus, although endogenous Zn^{2+} concentrations are similar in WT and ZnR/GPR39 KO colonocytes (Fig. 5A – B) and KCC1 expression levels are also similar in both genotypes (Fig. 5), upregulation of Cl^- transport is abolished in the absence of the ZnR/GPR39 receptor. This set of experiments therefore indicates that endogenous Zn^{2+} induces increased K^+/Cl^- transport, which is attenuated by EDTA. The complete recovery of K^+/Cl^- transport when excesses Zn^{2+} was applied in the presence of EDTA (Fig. 6C, E), suggests that this ion specifically enhanced transport activity. Moreover, Zn^{2+} acts via ZnR/GPR39 since the K^+/Cl^- transport is attenuated and is not sensitive to EDTA in ZnR/GPR39 KO tissue (Fig. 6D, E).

Finally, we asked whether ZnR/GPR39-dependent KCC1 activity is essential for reducing CTx-induced fluid accumulation. Fluid accumulation in WT mice treated with DIOA (500 μM 30 min before CTx treatment) was significantly increased compared to control mice, suggesting that KCC activity is essential for regulating water loss (Fig. 7A – B). In addition, treatment with DIOA completely abolished the effect of ZnR/GPR39, as the severity of fluid secretion in WT and ZnR/GPR39 KO mice was similar (Fig. 7B). This result suggests that reduced intestinal fluid accumulation in ZnR/GPR39-expressing mice is dependent on the activity of the basolateral KCC1.

3. Discussion

We report here that Zn^{2+} acting via a specific molecular target, ZnR/ GPR39, enhances K^+-dependent Cl^- absorption in colonic epithelial cells (Fig. 7C). This is strongly supported by the effect of inhibitors of the Gq dependent Ca^{2+} signal as well as MAPK pathway, which were previously shown to largely attenuate Zn^{2+}-dependent activation of ZnR/GPR39 signaling [19,20]. The specific role of ZnR/GPR39 is underscored by the loss of a Zn^{2+}-dependent effect in colonocytes from ZnR/GPR39 KO tissue, lacking GPR39 RNA or ZnR/GPR39 activity [32,44,58]. Taken together, the pH and the direct Cl^- transport measurements, both indicate that ZnR/GPR39 upregulates a K^+/Cl^- cotransporter to about 150% of its baseline activity. Similar upregulation of Cl^- transport by the farnesoid X receptor has been suggested as a potential anti-diarrheal pathway [6]. Here, the Cl^- transport is mediated by ZnR/GPR39-dependent upregulation of the activity of a basolaterally expressed KCC1. Our findings are supported by the Caco-2 cell model, where we show that pharmacological inhibition as well as siRNA silencing of KCC1, but not siKCC3 or siKCC4, largely abolish ZnR/GPR39-de-pendent activation of ion transport. The use of non-polarized Caco-2 cells allows us to dissect the molecular pathway and transfect the cells with the siRNA constructs, and thereby to elucidate the pathway activated by Zn^{2+} and ZnR/GPR39. The physiological relevance of this pathway is then revealed using colon tissue to show basolateral expression of the KCC1 and enhancement of ion transport triggered by transient luminal Zn^{2+} changes (only in ZnR/GPR39 expressing colonocytes). Net intestinal Cl^- secretion is dependent on the action of CFTR [59] in concert with basolateral transport

proteins that mediate uptake of Cl^- and K^+, including the Na^+/K^+ ATPase, $Na^+/K^+/2Cl^-$ cotransporter (i.e., NKCC1) [60] and basolateral K^+ channel [61]. A principle finding of this study is that mouse and human colonocytes express a functional KCC1 on the basolateral membrane. This cotransporter is a mediator of Cl^- efflux [62,63] and its basolateral expression suggests that it is an important player in net Cl^- absorption. This process can counteract luminal Cl^- secretion followed by fluid loss, which presents as diarrhea.

Numerous studies indicate that KCC transporters are regulated during physiological activity [63,64]. Our results show that Zn^{2+} enhanced K^+/Cl^- transport activity mediated by KCC1, and that ZnR/GPR39 is essential for this effect. The role of KCC was initially demonstrated using well-established pharmacological tools [48,50]. As such, the KCC inhibitor DIOA, used at two different concentrations, abolished Zn^{2+}-dependent upregulation of K^+/Cl^- transport but the NKCC inhibitor bumetanide did not reverse this effect. Higher concentrations of DIOA were suggested to inhibit the Na^+-dependent Na^+/K^+ ATPase [65], but further studies suggested that it may be an indirect effect of this compound [66,67]. Importantly, the effect of ZnR/GPR39 on ion transport persisted in the absence of Na^+ but was abolished in the absence of Cl^-, suggesting that a Na^+-dependent or Cl^--independent transporter are not likely regulated by ZnR/GPR39. Furthermore, silencing KCC1 eliminated the Zn^{2+}-dependent upregulation of K^+/Cl^- transport, specifically showing that this isoform of KCC1 is responsible for the Zn^{2+}-dependent Cl^- transport. Thus we suggest that the NKCC or the Na^+/K^+ ATPase were not involved in the Zn^{2+}-dependent upregulation of K^+/Cl^- transport. We show that ZnR/GPR39 activation induces KCC1 upregulation by an ERK1/2 (MAPK) dependent pathway. This result is consistent with previous studies showing that the neuronal KCC2 is up-regulated by PKC-dependent phosphorylation of serine 940 [68]. In addition, MAPK-dependent upregulation of KCC1 activity was shown in red blood cells [69,70]. In addition, synaptically-released Zn^{2+} activates ZnR/GPR39-dependent MAPK signaling that upregulates the neuronal KCC2 [44]. Further studies are required to decipher whether ZnR/ GPR39 directly modulates KCC activity or regulates its membrane localization, as previously described in neurons [44,71].

Chelation of luminal Zn^{2+} with EDTA attenuated ion transport in WT colon tissue but failed to affect transport in colon tissue from ZnR/ GPR39 KO mice. Addition of higher concentration of Zn^{2+} reversed the inhibitory effect of EDTA on KCC1 activity, indicating that this metal ion is specifically affecting the Cl^- transport, likely mediated by KCC. Moreover, baseline activity of the transporter in ZnR/GPR39 KO mice was significantly reduced compared to WT. These findings suggest that release of endogenous Zn^{2+} from the tissue itself is sufficient to elicit ZnR/GPR39 activation that is essential for baseline function of the K^+/Cl^- cotransporter. Release of Zn^{2+} from colon cells may be mediated by Zn^{2+} transporters, possibly ZnT6 [72], or during cell death [23], which occurs continuously in this tissue. We have previously shown that release of endogenous Zn^{2+} by Caco-2 cells is sufficient to induce ZnR/GPR39-dependent cell growth [24].

In previous studies, incubation of Caco-2 cells with Zn^{2+} on the serosal, but not mucosal, side reduced intestinal Cl^- secretion by blocking basolateral membrane K^+ channels or via regulation of cAMP or Ca^{2+}-dependent pathways [9,16,17,73]. These studies used very high concentration of Zn^{2+} (1 mM) or prolonged (>20 min) exposure, which likely induce

increases in intracellular Zn^{2+} levels and there by modulate multiple signaling pathways that regulate ion transport [74,75]. In contrast, we show here that upregulation of ion transport is induced by extracellular Zn^{2+}, via ZnR/GPR39 not only in Caco-2 cells but also in native colon tissues. Moreover, we show that Zn^{2+}, via an apical ZnR/GPR39 [24], upregulates a Cl^- absorptive mechanism that is attenuated by luminal application of the Zn^{2+} chelator EDTA. Thus, it is likely that serosal or intracellular Zn^{2+} activate a ZnR/GPR39-independent pathway to reduce Cl^- secretion; while ZnR/GPR39 upregulates KCC1 activity. A similar dual role for Zn^{2+} was demonstrated in neurons, where intracellular Zn^{2+} attenuated Cl^- transport [42], while extracellular Zn^{2+} via ZnR/GPR39 upregulated KCC2 activity and Cl^- efflux [44,71].

By upregulating KCC1 activity, Zn^{2+} and ZnR/GPR39 increase basolateral Cl^- transport, thereby contributing to net Cl^- absorption and reducing luminal secretion. Our finding of a basolateral Cl^- transporter, KCC1, provides a mechanism for absorption of this ion. In the context of diarrhea, this process slows intestinal water loss. A previous study has shown that incubation of Caco-2 cells with Zn^{2+}, at the serosal side, induced NHE3 upregulation [15] that can support a role for Zn^{2+} in enhancing Na^+ absorption and thereby reduction of diarrhea [5,35,36]. Interestingly, while the paradigm used in the current study does not involve acidification of the cells and therefore NHE activity is not monitored, we have previously shown that luminal Zn^{2+} upregulates Na^+/H^+ exchange activity in ZnR/GPR39 expressing Caco-2 and native tissue colonocytes [20,24]. It would be interesting to determine if prolonged exposure to serosal Zn^{2+} triggered ZnR/GPR39 activation or intracellular Zn^{2+} rise that regulated NHE3 activity and reduced diarrhea in the first study. Altogether, our data indicate that ZnR/GPR39 can reduce water loss by enhancing Na^+ absorption via an apical NHE3 and Cl^- absorption via a basolateral KCC1. Note that the major Na^+ absorptive process in the small intestine in fasting state is neutral NaCl absorption, importantly Zn^{2+} via ZnR/GPR39 stimulates transport of both components of this process suggesting a major role for this pathway also in intestinal physiology. Indeed, treatment with cholera toxin resulted in increased luminal fluid volume in ZnR/GPR39 KO compared to WT mice, an effect that was similar in its size to previous studies [6]. Interestingly, the Ca^{2+} sensing Gq-coupled receptor, CaR, was already linked to reduction of fluid secretion [76] triggered by CTx. We and others have shown that ZnR/GPR39 activity is distinct from the CaR mediated activity, and moreover that CaR is not activated by Zn^{2+} [19,20,77–79]. Moreover, CaR dependent regulation of Cl^- transport was clearly mediated by a bumetanide-sensitive NKCC while ZnR/GPR39 upregulated a KCC-dependent pathway. We have shown that ZnR/GPR39 and CaR may interact [25], and hence the compensatory mechanism observed in ZnR/GPR39 KO tissue or following chronic dietary Zn^{2+}-deficiency may be mediated by upregulation of CaR-dependent pathways.

ZnR/GPR39 provides a mechanistic explanation for the well-known beneficial effect of Zn^{2+} in treatment of diarrhea. Although the role of Zn^{2+} in diarrhea is well appreciated, the mechanisms underlying its action are not fully understood. The role of Zn^{2+} supplementation as a mean for the recovery of this micronutrient deficiency is important, especially under conditions of nutritional Zn^{2+} deficiency. Yet Zn^{2+} supplementation is also effective under Zn^{2+}-sufficient diet. Multiple intracellular proteins are regulated by Zn^{2+} and there are 24 transporters involved in Zn^{2+} homeostasis, which may all play a role in diarrhea

[18,80]. Such role for intracellular Zn^{2+} may underlie the effects of prolonged incubation at the serosal or mucosal sides [9,15–17] and may play an important role in situation of severe Zn^{2+} deficiency in humans. Our studies, using a very brief exposure of the cells to Zn^{2+}, link a specific extracellular Zn^{2+} sensing mechanism to regulation of signaling and ion transport that may offer an important and sensitive therapeutic target [19,26,33,34,81]. Indeed, we see a significant effect of ZnR/GPR39 knockdown on the fluid accumulation in the CTx model, and this is abolished in the absence of endogenous Zn^{2+} or KCC1 activity. Importantly, future studies should be aimed to determine if the net effect on fluid loss can be synergistically regulated by combined use of ZnR/ GPR39 inhibition, likely affecting KCC and NHE, as well as modulation of ZnR/GPR39 independent pathways, such as the NKCC or other Cl^- transporters [7,82,83]. We have shown the role of Zn^{2+} using chelation and rescue of the Zn^{2+}-dependent KCC1 activation in WT tissue but not in ZnR/GPR39 KO tissue. Moreover, we have used a Zn^{2+}-deficient diet to show that the effect of ZnR/GPR39 on fluid accumulation is lost. The use of a chronic Zn^{2+}-deficient diet is expected to lower the endogenous Zn^{2+} levels accumulated in cells [84] and therefore the release of endogenous Zn^{2+} for the activation of ZnR/GPR39. Further studies that will identify the source of endogenous Zn^{2+} that activates colonic ZnR/GPR39 will be essential to further link the effect of dietary Zn^{2+} on diarrhea even under conditions of sufficient dietary Zn^{2+}. While Zn^{2+} supplementation ameliorates diarrheal symptoms and shortens the recovery period [85], our study is the first step towards elucidating the underlying mechanism that may be of significance for optimizing the therapeutic process. For example: excess Zn^{2+} may actually desensitize ZnR/GPR39 [20], permeate the cell membrane, or affect other ion transport mechanisms [80], thereby reducing the benefits of Zn^{2+} treatment. Ultimately, identification of high affinity and specific agonists may provide a more efficient diarrheal treatment. Thus, our study identifies ZnR/GPR39 as a promising target for emerging specific therapeutic strategies to enhance ion absorption in patients with diarrhea.

4. Materials and methods

4.1. Cholera toxin-induced diarrhea model

All experimental procedures and protocols involving animals were approved by the committee for the Ethical Care and Use of Animal in Experiments at Ben-Gurion University of the Negev. Male $GPR39^{+/+}$ (WT) and $ZnR/GPR39^{-/-}$ (KO) littermates of C57BL background [58], genotyped as previously described [32], were maintained on normal diet (Harlan, Teklad Global 18, 70 ppm Zn^{2+}). At 10–12 weeks of age, mice were fed a 200 μl solution containing cholera toxin (CTx, 20 μg in 7% $NaHCO_3$) through an orogastric tube. Six hours later, the mice were sacrificed, the proximal duodenum and distal colon were tied off, and intestines removed. Intestinal secretions were collected and weighed, providing a diarrheal severity measure. To directly determine an effect by Zn^{2+}, a similar procedure was employed to WT and ZnR/GPR39 KO mice following four weeks of moderate-Zn^{2+} diet containing 30 ppm Zn^{2+} (Research Diets) or Zn^{2+}-deficient diet containing only 5 ppm Zn^{2+} (Research Diets). To determine the effect of ZnR/GPR39 dependent Cl^- transport/ absorption, 500 μM [(dihydroindenyl)oxy] alkanoic acid, DIOA [48] in 7% $NaHCO_3$ was delivered orally 30 min before CTx treatment.

4.2. Cell culture

Caco-2 cells were grown as previously described [86]. For imaging experiments, cells were seeded on 60-mM plates with coverslips and imaged following 48 h of incubation.

4.3. Fluorescent ion imaging

Fluorescent imaging measurements were acquired as described previously [24,44], using Imaging Workbench 5 (Indec, CA) and analyzed in Microsoft Excel. Cells were loaded with 1 μM of the H^+ indicator BCECF-AM [$2'$,$7'$-Bis-(2-Carboxyethyl)-5-(and-6)-Carboxyfluorescein, Acetoxymethyl Ester] (TEF-Labs) in 0.1% BSA in Ringer's. The rate of K^+/Cl^- transport was monitored by applying the NH_4Cl paradigm [20, 44]. While radioactive ions have been traditionally used to monitor the activity of the Cl^- transporters, the fluorescent based live-imaging system allows similar analysis of net ion flux/accumulation with a very good temporal resolution in specific cells. Indeed, this paradigm has been well established in numerous papers [42–44,55,87,88]. Briefly, cells were perfused with Ringer's solution (containing 120 mM NaCl, 5.4 mM KCl, 0.8 mM $MgCl_2$, 20 mM HEPES, 15 mM glucose, 1.5 mM $CaCl_2$ at pH 7.4) to obtain a stable baseline. Then, K^+-free Ringer's solution containing NH_4Cl (10 mM) was added and induced alkalization due to passive entry of NH_3 into the cells that when equilibrated with NH_4^+, in the presence of water, binds H^+ ions within the cytoplasm. This was then followed by acidification of the cells caused by influx of extracellular NH_4^+, which serves as a surrogate to K^+, mediated by NKCC/KCC cotransporters acting in normal or reverse mode driven by the NH_4^+ gradient [44]. Briefly, the NH_4^+ influx requires re-adjustment of the equilibrium with NH_3, thus inducing more NH_4^+ breakdown within the cytoplasm, and therefore cellular acidification occurs. In some experiments a Cl^--free solution was used for superfusion of the cells (sodium gluconate replacing NaCl in HEPES buffered solution) and 10 mM $(NH_4)2HPO_4$ at pH 7.4 was applied, resulting in alkalinization of the cytoplasm as described above. Fluorescent BCECF signals are represented as a ratio, R, of the signal obtained using excitation of 470 nm/440 nm and 510 nm emission bandpass filters (Chroma Technology).

Rates of steady state NH_4^+ influx represent NKCC/KCC activity, and were determined by monitoring the initial 70 s period of acidification. Since NH_3 permeation rates may differ between coverslips, the rate of acidification was monitored from the time when maximal signal was reached per coverslip [44]. Rates of acidification, NKCC/KCC activity, were averaged per set of experiments and are presented in the bar graphs. To monitor the Cl^- transport directly, cells were loaded with 5 mM MQAE (*N*-(ethoxycarbonylmethyl)-6-methoxy-quinolinium bromide) in 0.1% K^+ free Ringer's solution for 1 h at 37 °C and washed for 30 min in the presence or absence of DIOA (40 μM). The rate of K^+/Cl^- transport was monitored by applying KCl (20 mM) to the cells, thus reversing KCC activity, which results in Cl^- influx into the cells and quenching of MQAE fluorescence [42], measured using 360 nm excitation/ 510 nm bandpass emission filters and normalized to baseline fluorescence signal (F/F_0). Initial rates of MQAE fluorescence change (35 s following the initial decrease in fluorescence) were determined to represent ion transport rates. All results shown are representative traces from one slide showing the averaged

responses of 9–25 cells. Bar graphs exhibit the mean response of 'n' slides taken from at least 3 independent experiments.

To study the effect of ZnR/GPR39, cells were treated with 100 μM Zn^{2+} for 1 min. At this concentration, Zn^{2+} activates the ZnR/GPR39 but, does not significantly change the level of intracellular Zn^{2+} [23]. Measurements of intracellular Zn^{2+} and Ca^{2+} levels in Caco-2 cells were performed using cells loaded with FluoZin3 or Fura-2, as previously described [32,33,44,55].

4.4. Ion transport in colon tissues

~5 cm of distal colon from WT and ZnR/GPR39 KO mice were washed with Parson's solution using a plastic syringe. A longitudinal incision was made along the colon wall and the tissue (maintained at 4 °C) was spread keeping the mucosal-luminal side upwards on coverslips using cyanoacrylate glue [89]. Coverslips were transferred to high K^+ solution at room temperature for subsequent treatment. To chelate luminal Zn^{2+}, all solutions contained 100 μM ethylenediaminetetraacetic acid (EDTA). Luminal Ca^{2+} levels are not influenced by this concentration of EDTA that has higher affinity to Zn^{2+} than to Ca^{2+}. Colon segments with the epithelial layer facing upward were loaded with BCECF (5 μM, 30 min) in Ringer's solution and the NH_4Cl paradigm was applied [20].

4.5. Fluorescent Zn^{2+} imaging

For imaging vesicular Zn^{2+}, cryostat sections (30 μm) through the colon were loaded with the Zn^{2+}-selective dye Zinpyr-1 (20 μM, Santa Cruz Biotechnology) for 5 min, as previously described [53]. Images were recorded (40×, Olympus FluoView, FV1000) every 5 min. Fluorescence intensity was analyzed using Photoshop 8. Briefly, a threshold reference was applied to each series of images and the general intensity in regions of interest was determined as a function of time. The relative fluorescence level was normalized to the initial value (F/F_0) as used for non-ratiometric dyes.

4.6. Silencing of KCC1, KCC3 and KCC4 cotransporters

Caco-2 cells seeded at 80–90% confluence were transfected using Lipofectamine 2000 (Invitrogen), and used for the different experimental settings 48 h post transfection. The transfection efficiency, as monitored using YFP-expressing representative slides was 40–50% of the total cells. The target protein constructs (Sigma-Aldrich) were: siKCC1 (against NM_005072.4, NM_001145961.1, NM_001145962.1, NM_001145963.1, NM_001145964.1 variants): forward primer CAUCUUCUUCCCUUCUGUA. siKCC3 (against NM_133647.1, NM_005135.2, NM_0010 42494.1, NM_001042495.1, NM_001042496.1, NM_001042497.1 variants): forward primer CGGACAUAAGAAAGCUCGA. siKCC4 (NM_006598.2): forward primer GGUGGAACAAGAGAGCUUC. siRNA control (scrambled): forward primer GCCCAGAUCCCUGUACGU. Total RNA was purified using RNeasy Mini Kit as described by the manufacturer (Qiagen). Purified RNA (1 μg) was converted to cDNA using synthesis Kit (Life Technologies). The cDNA was used for PCR analysis with the Red load TaqMaster (Larova) and primers supplied by Sigma-Aldrich: KCC1 (recognizes all variants): forward: TGGGACCATTTTCCTGACC reverse:

CATGCTTCTCCACGATGTCAC; KCC3 (recognizes all variants): forward: GCCCGAAACACAAAATCACT reverse: GGATACCTGGGGGAAGATGT; KCC4: forward: GACTCGTTTCCGCAAAACC reverse: AGAGTGCCGTGATGCTGTTGG. The same cDNA was diluted at 1:5 and subjected to real time PCR procedure (Taqmen, Applied Biosystems), which was done with ABsolute Blue QPCR kit (Thermo Scientific). Required primers and probes were predesigned and supplied by Solaris: KCC1 (recognizes 1,2,4,5,6 variants): forward: CTGGCACTGTTTGAGGAAGA reverse: GCTTTCCCAGAAGAGACGAT probe: TCCGCCCAAAGGTATCG; KCC3 (recognizes all variants): forward: CCTAATGGCTGGCGTCAA reverse: ATGGGCAGCAGTTGTCACTC probe: CTT TTATTGGCACAGTTCG; KCC4 forward: TACCTGGACAAGCACATGGA reverse: GCT CATTAGGGACCGTAT probe: GCGGGCCGAGGAGAACATAC. Western blot analysis to determine protein levels was performed as described [25]. Extracted proteins (50 μg) were separated on 7.5% SDS–PAGE followed by immunoblotting using antibodies against KCC1 (1:1000, LifeSpan BioSciences), β-actin (1:40,000, MP Biomedicals) and KCC3 (1:5000, Santa Cruz Biotechnology). Densitometric analysis was performed using EZQuant. The values presented are normalized to β-actin.

4.7. Immunofluorescence

Localization of KCC1 in colon tissues from WT and ZnR/GPR39 KO mice or human colon tissues was detected by immunofluorescence confocal microscopy (Olympus FluoView or Zeiss LSM 510 Meta). Tissues were fixed with 4% paraformaldehyde, and after heat induced antigen retrieval (95 °C, 10 min) the tissues were incubated overnight at 4 °C with primary KCC1 antibody (LS-B2377, LifeSpan BioSciences), and co-stained with Na^+/K^+ ATPase antibodies (Abcam) and secondary Cy3-and Cy2-conjugated antibodies. For competition assay, the KCC1 antibodies were incubated in the presence of a blocking peptide (LS-E26489) or control non-specific peptide containing solution. Negative control slides were treated with only the secondary antibodies which showed virtually blank images. The peptide blocking and the negative control showed that KCC1 is not detected in a non-specific manner. Several independent batches of the antibody exhibited similar staining of KCC1, indicating it is reproducible. Taken together with the immunoblot experiments, showing similar level of protein downregulation in siKCC1 silenced cells as the mRNA (Fig. 3), this analysis suggests that the KCC1 antibody specifically interacted with the protein. Quantification of the distribution of KCC1 was obtained by using Photoshop 8, by applying a common threshold and measuring the mean intensity of the pixels, normalized to that of Na^+/K^+ ATPase from the same slice. Co-localization of these proteins was analyzed (ImageJ, NIH) using "Mandar" overlap coefficient [90].

4.8. Statistical analysis

Data are expressed as means ± SEM. Each treatment was compared with the control or Zn^{2+} treatment, and statistical significance between the groups determined using the Student's t-test or ANOVA with post hoc Tukey test as appropriate. *, $p < 0.05$ and **, $p < 0.01$ and ***, $p < 0.001$.

Supplementary Material

Refer to Web version on PubMed Central for supplementary material.

Acknowledgments

References

1. Fischer Walker CL, Black RE. Micronutrients and diarrheal disease. Clin Infect Dis. 2007; 45(Suppl. 1):S73–S77. [PubMed: 17582575]

2. Kulkarni H, Mamtani M, Patel A. Roles of zinc in the pathophysiology of acute diarrhea. Curr. Infect Dis. Rep. 2012; 14(1):24–32. [PubMed: 22167529]

3. Berkes J, Viswanathan VK, Savkovic SD, Hecht G. Intestinal epithelial responses to enteric pathogens: effects on the tight junction barrier, ion transport and inflammation. Gut. 2003; 52(3): 439–451. [PubMed: 12584232]

4. Bachmann O, Seidler U. News from the end of the gut—how the highly segmental pattern of colonic HCO transport relates to absorptive function and mucosal integrity. Biol. Pharm. Bull. 2011; 34(6): 794–802. [PubMed: 21628874]

5. Thiagarajah JR, Ko EA, Tradtrantip L, Donowitz M, Verkman AS. Discovery and development of antisecretory drugs for treating diarrheal diseases. Clin. Gastroenterol. Hepatol. 2014; 12(2):204–209. [PubMed: 24316107]

6. Mroz MS, et al. Farnesoid X receptor agonists attenuate colonic epithelial secretory function and prevent experimental diarrhoea in vivo. Gut. 2014; 63(5):808–817. [PubMed: 23916961]

7. Thiagarajah JR, Donowitz M, Verkman AS. Secretory diarrhoea: mechanisms and emerging therapies. Nat Rev. Gastroenterol. Hepatol. 2015; 12(8):446–457. [PubMed: 26122478]

8. Sazawal S, et al. Zinc supplementation in young children with acute diarrhea in India. N. Engl. J. Med. 1995; 333(13):839–844. [PubMed: 7651474]

9. Hoque KM, Rajendran VM, Binder HJ. Zinc inhibits cAMP-stimulated Cl secretion via basolateral K-channel blockade in rat ileum. Am. J. Physiol. Gastrointest Liver Physiol. 2005; 288(5):G956–G963. [PubMed: 15618279]

10. Bhutta ZA, et al. Therapeutic effects of oral zinc in acute and persistent diarrhea in children in developing countries: pooled analysis of randomized controlled trials. Am. J. Clin. Nutr. 2000; 72(6):1516–1522. [PubMed: 11101480]

11. Crisinel PA, et al. Demonstration of the effectiveness of zinc in diarrhoea of children living in Switzerland. Eur. J. Pediatr. 2015; 174(8):1061–1067. [PubMed: 25749908]

12. Passariello A, et al. Efficacy of a new hypotonic oral rehydration solution containing zinc and prebiotics in the treatment of childhood acute diarrhea: a randomized controlled trial. J. Pediatr. 2011; 158(2):288–292. e281. [PubMed: 20828714]

13. Walker CL, Black RE. Zinc for the treatment of diarrhoea: effect on diarrhoea morbidity, mortality and incidence of future episodes. Int. J. Epidemiol. 2010; 39(Suppl. 1):i63–i69. [PubMed: 20348128]

14. Hoque KM, Binder HJ. Zinc in the treatment of acute diarrhea: current status and assessment. Gastroenterology. 2006; 130(7):2201–2205. [PubMed: 16762641]

15. Hoque KM, Sarker R, Guggino SE, Tse CM. A new insight into pathophysiological mechanisms of zinc in diarrhea. Ann. N. Y. Acad. Sci. 2009; 1165:279–284. [PubMed: 19538317]

16. Berni Canani R, et al. Zinc inhibits calcium-mediated and nitric oxide-mediated ion secretion in human enterocytes. Eur. J. Pharmacol. 2010; 626(2–3):266–270. [PubMed: 19819236]

17. Canani RB, et al. Zinc inhibits cholera toxin-induced, but not *Escherichia coli* heat-stable enterotoxin-induced ion secretion in human enterocytes. J. Infect. Dis. 2005; 191(7):1072–1077. [PubMed: 15747242]

18. Berni Canani R, Buccigrossi V, Passariello A. Mechanisms of action of zinc in acute diarrhea. Curr. Opin. Gastroenterol. 2011; 27(1):8–12. [PubMed: 20856116]

19. Hershfinkel M, Moran A, Grossman N, Sekler I. A zinc-sensing receptor triggers the release of intracellular $Ca2^+$ and regulates ion transport. Proc. Natl. Acad. Sci. U. S. A. 2001; 98(20):11749–11754. [PubMed: 11573009]

20. Azriel-Tamir H, Sharir H, Schwartz B, Hershfinkel M. Extracellular zinc triggers ERK-dependent activation of Na^+/H^+ exchange in colonocytes mediated by the zinc-sensing receptor. J. Biol. Chem. 2004; 279(50):51804–51816. [PubMed: 15355987]

21. Dubi N, Gheber L, Fishman D, Sekler I, Hershfinkel M, et al. Extracellular zinc zinc-citrate acting through a putative zinc-sensing receptor regulate growth and survival of prostate cancer cells. Carcinogenesis. 2008; 29(9):1692–1700. [PubMed: 18310092]

22. Besser L, et al. Synaptically released zinc triggers metabotropic signaling via a zinc-sensing receptor in the hippocampus. J. Neurosci. 2009; 29(9):2890–2901. [PubMed: 19261885]

23. Sharir H, Zinger A, Nevo A, Sekler I, Hershfinkel M, et al. Zinc released from injured cells is acting via the $Zn2^+$-sensing receptor ZnR to trigger signaling leading to epithelial repair. J. Biol. Chem. 2010; 285(34):26097–26106. [PubMed: 20522546]

24. Cohen L, Asraf H, Sekler I, Hershfinkel M. Extracellular pH regulates zinc signaling via an Asp residue of the zinc-sensing receptor (ZnR/GPR39). J. Biol. Chem. 2012; 287(40):33339–33350. [PubMed: 22879599]

25. Asraf H, et al. The ZnR/GPR39 interacts with the CaSR to enhance signaling in prostate and salivary epithelia. J. Cell Physiol. 2013

26. Hershfinkel, M. The zinc-sensing receptor, ZnR/GPR39: signaling and significance. In: Fukada, T., Kambe, T., editors. Zinc Signals in Cellular Functions and Disorders. Springer; Japan: 2014. p. 11-134.

27. Popovics P, Stewart AJ. GPR39: a Zn(2+)-activated G protein-coupled receptor that regulates pancreatic gastrointestinal and neuronal functions. Cell. Mol. Life Sci. 2011; 68(1):85–95. [PubMed: 20812023]

28. Yasuda S, et al. Isolation of $Zn2^+$ as an endogenous agonist of GPR39 from fetal bovine serum. J. Recept. Signal Transduct. Res. 2007; 27(4):235–246. [PubMed: 17885920]

29. Holst B, et al. GPR39 signaling is stimulated by zinc ions but not by obestatin. Endocrinology. 2007; 148(1):13–20. [PubMed: 16959833]

30. Lauwers E, Landuyt B, Arckens L, Schoofs L, Luyten W. Obestatin does not activate orphan G protein-coupled receptor GPR39. Biochem. Biophys. Res. Commun. 2006; 351(1):21–25. [PubMed: 17054911]

31. Zhang JV, et al. Obestatin a peptide encoded by the ghrelin gene, opposes ghrelin's effects on food intake. Science. 2005; 310(5750):996–999. [PubMed: 16284174]

32. Cohen L, Azriel-Tamir H, Arotsker N, Sekler I, Hershfinkel M. Zinc sensing receptor signaling, mediated by GPR39, reduces butyrate-induced cell death in HT29 colonocytes via upregulation of clusterin. PLoS One. 2012; 7(4):e35482. [PubMed: 22545109]

33. Cohen L, Sekler I, Hershfinkel M. The zinc sensing receptor, ZnR/GPR39, controls proliferation and differentiation of colonocytes and thereby tight junction formation in the colon. Cell Death Dis. 2014; 5:e1307. [PubMed: 24967969]

34. Sunuwar L, Medini M, Cohen L, Sekler I, Hershfinkel M. The zinc sensing receptor, ZnR/GPR39, triggers metabotropic calcium signalling in colonocytes and regulates occludin recovery in experimental colitis. Philos. Trans. R. Soc. Lond. Ser. B Biol. Sci. 2016; 371(1700)

35. Donowitz M, Ming Tse C, Fuster D. SLC9/ NHE gene family a plasma membrane and organellar family of Na(+)/H(+) exchangers. Mol. Asp. Med. 2013; 34(2–3):236–251.

36. Malo ME, Fliegel L. Physiological role and regulation of the Na^+/H^+ exchanger. Can. J. Physiol. Pharmacol. 2006; 84(11):1081–1095. [PubMed: 17218973]

37. Huang ZL, Dufner-Beattie J, Andrews GK. Expression and regulation of SLC39A family zinc transporters in the developing mouse intestine. Dev. Biol. 2006; 295(2):571–579. [PubMed: 16682017]

38. Suh SW, et al. Decreased brain zinc availability reduces hippocampal neurogenesis in mice and rats. J. Cereb. Blood Flow Metab. 2009; 29(9):1579–1588. [PubMed: 19536073]

39. Andrews GK. Regulation and function of Zip4, the acrodermatitis enteropathica gene. Biochem. Soc. Trans. 2008; 36(Pt 6):1242–1246. [PubMed: 19021533]

40. Dufner-Beattie J, Huang ZL, Geiser J, Xu W, Andrews GK. Generation and characterization of mice lacking the zinc uptake transporter ZIP3. Mol. Cell. Biol. 2005; 25(13):5607–5615. [PubMed: 15964816]

41. Dufner-Beattie J, Kuo YM, Gitschier J, Andrews GK. The adaptive response to dietary zinc in mice involves the differential cellular localization and zinc regulation of the zinc transporters ZIP4 and ZIP5. J. Biol. Chem. 2004; 279(47):49082–49090. (Epub 42004 Sep 49089). [PubMed: 15358787]

42. Hershfinkel M, et al. Intracellular zinc inhibits KCC2 transporter activity. Nat. Neurosci. 2009; 12(6):725–727. [PubMed: 19430470]

43. Titz S, Hormuzdi S, Lewen A, Monyer H, Misgeld U. Intracellular acidification in neurons induced by ammonium depends on KCC2 function. Eur. J. Neurosci. 2006; 23(2):454–464. [PubMed: 16420452]

44. Chorin E, et al. Upregulation of KCC2 activity by zinc-mediated neurotransmission via the mZnR/ GPR39 receptor. J. Neurosci. 2011; 31(36):12916–12926. [PubMed: 21900570]

45. Ganay T, et al. Regulation of neuronal pH by the metabotropic zinc receptor mZnR/ GPR39. J. Neurochem. 2015

46. Haas M, Forbush B 3rd. The Na-K-Cl cotransporter of secretory epithelia. Annu. Rev. Physiol. 2000; 62:515–534. [PubMed: 10845101]

47. Mercado A, Song L, Vazquez N, Mount DB, Gamba G. Functional comparison of the K^+-Cl^- cotransporters KCC1 and KCC4. J. Biol. Chem. 2000; 275(39):30326–30334. [PubMed: 10913127]

48. Garay RP, Nazaret C, Hannaert PA, Cragoe EJ Jr. Demonstration of a $[K^+,Cl^-]$-co-transport system in human red cells by its sensitivity to [(dihydroindenyl)oxy]alkanoic acids: regulation of cell swelling and distinction from the bumetanide-sensitive $[Na^+,K^+,Cl^-]$-cotransport system. Mol. Pharmacol. 1988; 33(6):696–701. [PubMed: 3380083]

49. Plata C, Meade P, Vazquez N, Hebert SC, Gamba G. Functional properties of the apical Na^+-K^+-$2Cl^-$ cotransporter isoforms. J. Biol. Chem. 2002; 277(13):11004–11012. [PubMed: 11790783]

50. Sun YT, Shieh CC, Delpire E, Shen MR. K(+)-Cl(−) cotransport mediates the bactericidal activity of neutrophils by regulating NADPH oxidase activation. J. Physiol. 2012; 590(14):3231–3243. [PubMed: 22526882]

51. Zhu L, Lovinger D, Delpire E. Cortical neurons lacking KCC2 expression show impaired regulation of intracellular chloride. J. Neurophysiol. 2005; 93(3):1557–1568. [PubMed: 15469961]

52. Lu J, Karadsheh M, Delpire E. Developmental regulation of the neuronal-specific isoform of K-Cl cotransporter KCC2 in postnatal rat brains. J. Neurobiol. 1999; 39(4):558–568. [PubMed: 10380077]

53. Giblin LJ, et al. Zinc-secreting Paneth cells studied by ZP fluorescence. J. Histochem. Cytochem. 2006; 54(3):311–316. [PubMed: 16260591]

54. Burdette SC, Walkup GK, Spingler B, Tsien RY, Lippard SJ. Fluorescent sensors for Zn(2+) based on a fluorescein platform: synthesis properties and intracellular distribution. J. Am. Chem. Soc. 2001; 123(32):7831–7841. [PubMed: 11493056]

55. Gilad D, et al. Homeostatic regulation of KCC2 activity by the zinc receptor mZnR/ GPR39 during seizures. Neurobiol. Dis. 2015

56. Larson AA, Kitto KF. Manipulations of zinc in the spinal cord by intrathecal injection of zinc chloride, disodium-calcium-EDTA or dipicolinic acid alter nociceptive activity in mice. J. Pharmacol. Exp. Ther. 1997; 282(3):1319–1325. [PubMed: 9316841]

57. Aiba I, Carlson AP, Sheline CT, Shuttleworth CW. Synaptic release and extracellular actions of Zn2$^+$ limit propagation of spreading depression and related events in vitro and in vivo. J. Neurophysiol. 2012; 107(3):1032–1041. [PubMed: 22131381]

58. Moechars D, et al. Altered gastrointestinal and metabolic function in the GPR39-obestatin receptor-knockout mouse. Gastroenterology. 2006; 131(4):1131–1141. [PubMed: 17030183]

59. Verkman AS, Lukacs GL, Galietta LJ. CFTR chloride channel drug discovery—inhibitors as antidiarrheals and activators for therapy of cystic fibrosis. Curr. Pharm. Des. 2006; 12(18):2235–2247. [PubMed: 16787252]

60. Reynolds A, et al. Dynamic and differential regulation of NKCC1 by calcium and cAMP in the native human colonic epithelium. J. Physiol. 2007; 582(Pt 2):507–524. [PubMed: 17478539]

61. Sorensen MV, Matos JE, Praetorius HA, Leipziger J. Colonic potassium handling. Pflugers Arch. 2010; 459(5):645–656. [PubMed: 20143237]

62. Sangan P, Brill SR, Sangan S, Forbush B 3rd, Binder HJ. Basolateral K-Cl cotransporter regulates colonic potassium absorption in potassium depletion. J. Biol. Chem. 2000; 275(40):30813–30816. [PubMed: 10878016]

63. Adragna NC, Di Fulvio M, Lauf PK. Regulation of K-Cl cotransport: from function to genes. J. Membr. Biol. 2004; 201(3):109–137. [PubMed: 15711773]

64. Gagnon KB, England R, Delpire E. Volume sensitivity of cation-Cl$^-$ cotransporters is modulated by the interaction of two kinases: Ste20-related proline-alanine-rich kinase and WNK4. Am. J. Phys. Cell Physiol. 2006; 290(1):C134–C142.

65. Fujii T, et al. Inhibition of P-type ATPases by [(dihydroindenyl)oxy]acetic acid (DIOA) a K$^+$-Cl$^-$ cotransporter inhibitor. Eur. J. Pharmacol. 2007; 560(2–3):123–126. [PubMed: 17303113]

66. Fujii T, Fujita K, Shimizu T, Takeguchi N, Sakai H. The NH(2)-terminus of K(+)-Cl(−) cotransporter 3a is essential for up-regulation of Na(+),K(+)-ATPase activity. Biochem. Biophys. Res. Commun. 2010; 399(4):683–687. [PubMed: 20691666]

67. Fujii T, et al. K$^+$-Cl$^-$ cotransporter-3a up-regulates Na$^+$,K$^+$-ATPase in lipid rafts of gastric luminal parietal cells. J. Biol. Chem. 2008; 283(11):6869–6877. [PubMed: 18178552]

68. Lee HH, et al. Direct protein kinase C-dependent phosphorylation regulates the cell surface Stability and activity of the potassium chloride cotransporter KCC2. J. Biol. Chem. 2007; 282(41):29777–29784. [PubMed: 17693402]

69. Gonsalves CS, et al. Angiogenic growth factors augment K-Cl cotransporter expression in erythroid cells via hypoxia-inducible factor-1 alpha. Am. J. Hematol. 2014; 89(3):273–281. [PubMed: 24227191]

70. Capo-Aponte JE, et al. Functional and molecular characterization of multiple K-Cl cotransporter isoforms in corneal epithelial cells. Exp. Eye Res. 2007; 84(6):1090–1103. [PubMed: 17418819]

71. Saadi RA, et al. SNARE-dependent upregulation of potassium chloride co-transporter 2 activity after metabotropic zinc receptor activation in rat cortical neurons in vitro. Neuroscience. 2012; 210:38–46. [PubMed: 22441041]

72. Yu YY, Kirschke CP, Huang L. Immunohistochemical analysis of ZnT1 4, 5 6 and 7 in the mouse gastrointestinal tract. J. Histochem. Cytochem. 2007; 55(3):223–234. [PubMed: 17101726]

73. Medani M, et al. Zinc sulphate attenuates chloride secretion in human colonic mucosae in vitro. Eur. J. Pharmacol. 2012; 696(1–3):166–171. [PubMed: 23022335]

74. Wilson M, Hogstrand C, Maret W. Picomolar concentrations of free zinc(II) ions regulate receptor protein-tyrosine phosphatase beta activity. J. Biol. Chem. 2012; 287(12):9322–9326. [PubMed: 22275360]

75. Maret W. New perspectives of zinc coordination environments in proteins. J. Inorg. Biochem. 2012; 111:110–116. [PubMed: 22196021]

76. Geibel J, et al. Calcium-sensing receptor abrogates secretagogue-induced increases in intestinal net fluid secretion by enhancing cyclic nucleotide destruction. Proc. Natl. Acad. Sci. U. S. A. 2006; 103(25):9390–9397. [PubMed: 16760252]

77. Saidak Z, Brazier M, Kamel S, Mentaverri R. Agonists and allosteric modulators of the calcium-sensing receptor and their therapeutic applications. Mol. Pharmacol. 2009; 76(6):1131–1144. [PubMed: 19779033]

78. Riccardi D. Cell surface Ca2$^+$(cation)-sensing receptor(s): one or many? Cell Calcium. 1999; 26(3–4):77–83. [PubMed: 10598270]

79. Smith JB, Dwyer SD, Smith L. Cadmium evokes inositol polyphosphate formation and calcium mobilization. Evidence for a cell surface receptor that cadmium stimulates and zinc antagonizes. J. Biol. Chem. 1989; 264(13):7115–7118. [PubMed: 2540174]

80. Sekler I, Sensi SL, Hershfinkel M, Silverman WF. Mechanism and regulation of cellular zinc transport. Mol. Med. 2007; 13(7–8):337–343. [PubMed: 17622322]

81. Hershfinkel, M. Zinc, a dynamic signaling molecule. In: Tamas, M.Klomp, L., Martinoia, E., editors. Molecular Biology of Metal Homeostasis and Detoxification, Topics in Current Genetics. 2006.

82. Bachmann O, et al. Expression and regulation of the Na$^+$-K$^+$-2Cl$^-$ cotransporter NKCC1 in the normal and CFTR-deficient murine colon. J. Physiol. 2003; 549(Pt 2):525–536. [PubMed: 12692180]

83. Singh V, et al. Translating molecular physiology of intestinal transport into pharmacologic treatment of diarrhea: stimulation of Na$^+$ absorption. Clin. Gastroenterol. Hepatol. 2014; 12(1): 27–31. [PubMed: 24184676]

84. Takeda A, Takefuta S, Okada S, Oku N. Relationship between brain zinc and transient learning impairment of adult rats fed zinc-deficient diet. Brain Res. 2000; 859(2):352–357. [PubMed: 10719084]

85. Hambidge KM. Zinc and diarrhea. Acta Paediatr. Suppl. 1992; 381:82–86. [PubMed: 1421947]

86. Wootten D, Christopoulos A, Sexton PM. Emerging paradigms in GPCR allostery: implications for drug discovery. Nat. Rev. Drug Discov. 2013; 12(8):630–644. [PubMed: 23903222]

87. Liu W, et al. Role of NKCC in BK channel-mediated net K(+) secretion in the CCD. Am. J. Phys. Renal Phys. 2011; 301(5):F1088–F1097.

88. Heitzmann D, et al. Regulation of the Na$^+$2Cl$^-$ K$^+$ cotransporter in isolated rat colon crypts. Pflugers Arch. 2000; 439(3):378–384. [PubMed: 10650991]

89. Schultheiss G, Lan Kocks S, Diener M. Methods for the study of ionic currents and Ca2$^+$-signals in isolated colonic crypts. Biol. Proc. Online. 2002; 3:70–78.

90. Dunn KW, Kamocka MM, McDonald JH. A practical guide to evaluating colocalization in biological microscopy. Am. J. Phys. Cell Physiol. 2011; 300(4):C723–C742.
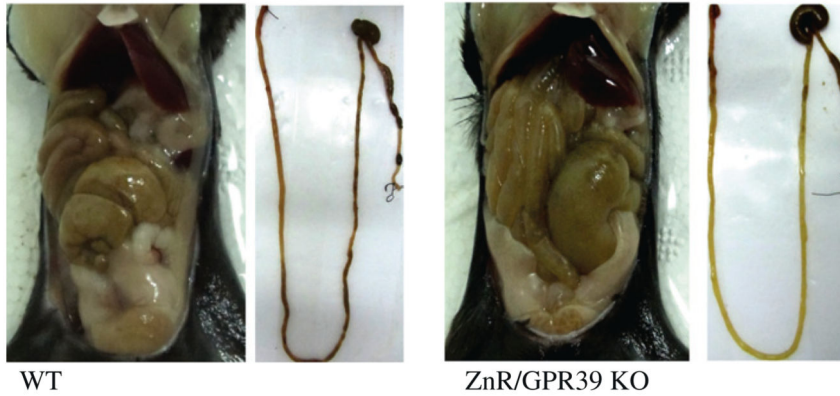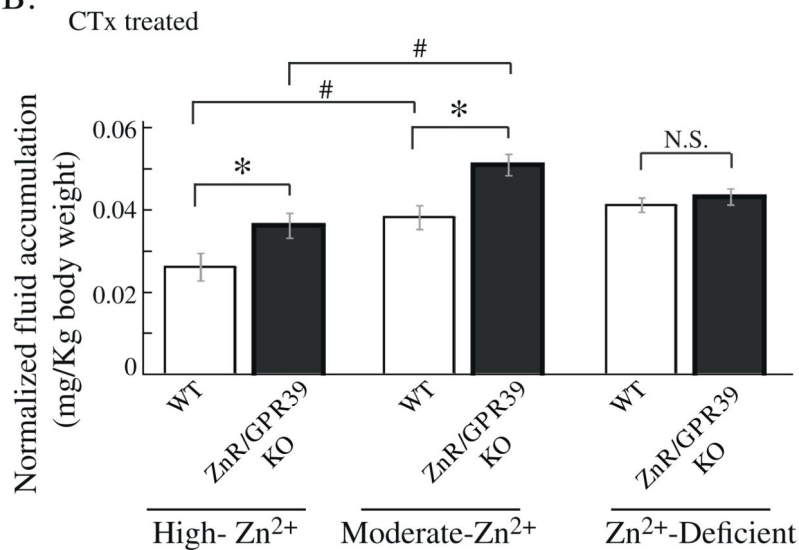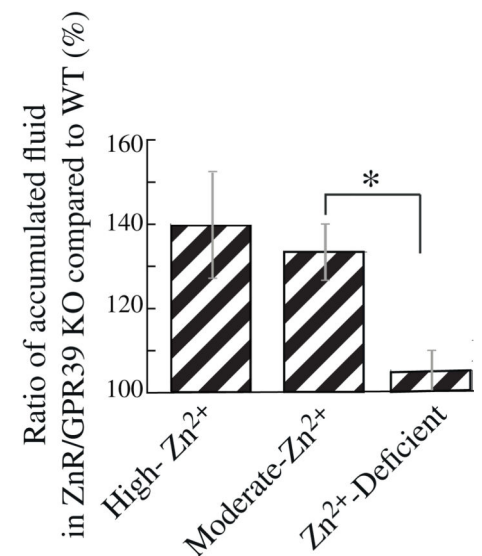
Fig 1.
Cholera-toxin induced intestinal fluid secretion is increased in the absence of ZnR/GPR39. (A) Mouse intestines, from the proximal duodenum to the mid-colon, from WT and ZnR/GPR39 KO mice following 6 h of gavage with cholera-toxin CTx. (B) Intestinal secretion content, normalized to body weight, 6 h following CTx treatment of WT or ZnR/GPR39 KO mice fed high-Zn^{2+} (n = 6), moderate Zn^{2+} (n = 6) or Zn^{2+}-deficient (n = 8) diet for 4 weeks. Note that the moderate Zn^{2+} diet induced a significant increase in fluid accumulation. (* p 0.05 compared to WT with same diet; # p 0.05 compared to mice fed high Zn^{2+} diet; mean ± SEM) (C) The ratio of normalized secretion content in ZnR/GPR39 KO mice compared to WT mice, presented as percentage (average WT secretion content for each diet = 100%, each data point is normalized to the average value). This analysis allows clear representation of the differences between the groups indicating that the ZnR/GPR39 KO mice have significantly larger secretion compared to the WT mice treated with the same diet. The bar diagrams represent mean ± SEM. (* p 0.05 compared to increase of accumulated fluid in mice fed moderate Zn^{2+} diet; mean ± SEM).
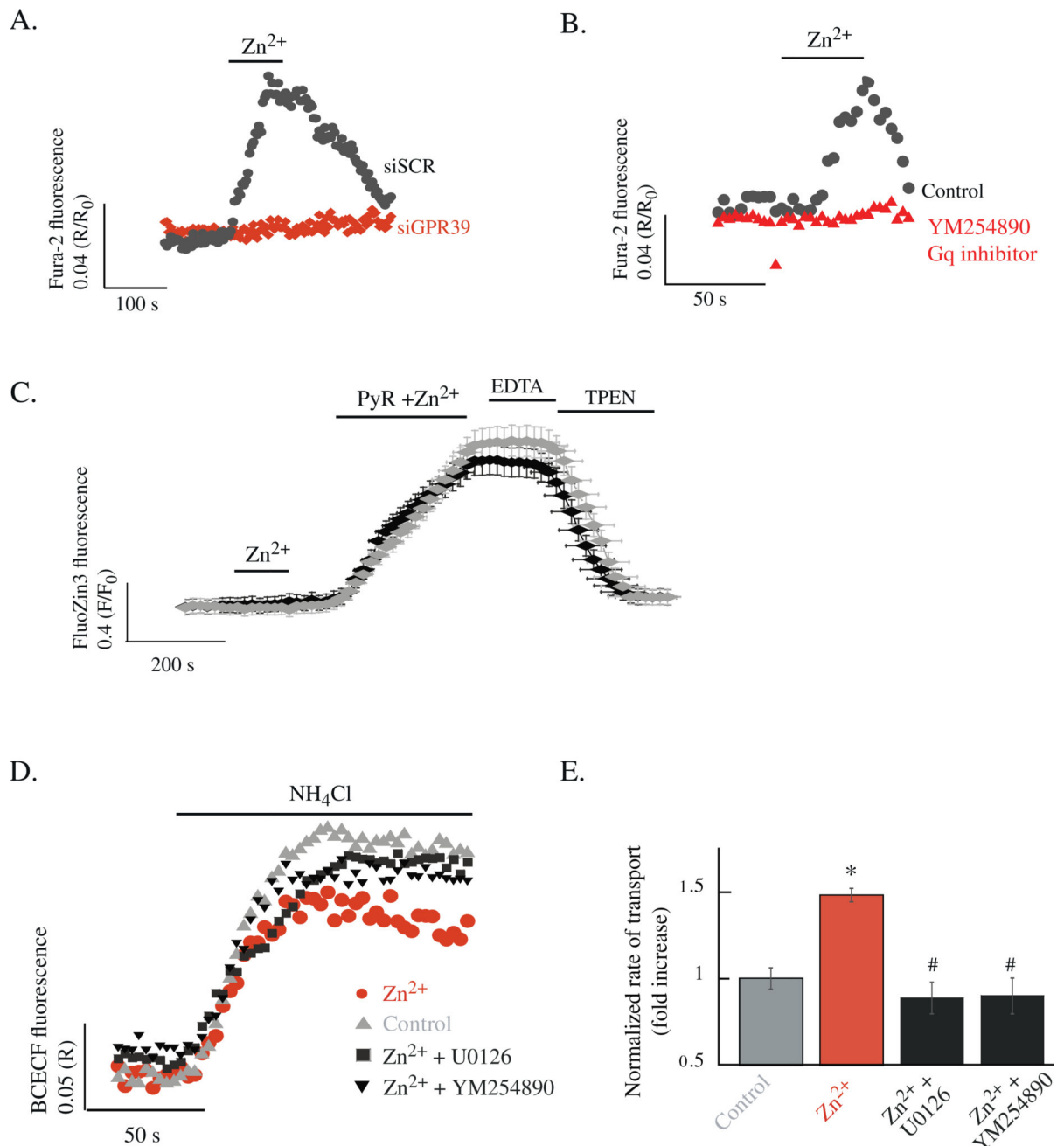
Fig 2.
Zn^{2+} activates ZnR/GPR39-dependent Ca^{2+} signaling and upregulates ion ctransport activity via the MAPK pathway in Caco-2 cells. (A) Representative averaged Ca^{2+} response of Caco-2 cells loaded with Fura-2 AM and transfected with a siRNA construct aimed to silence GPR39 (siGPR39, (33)) or scrambled (siSCR), loaded with Fura-2. Zn^{2+} (100 μM) was applied at the indicated time. (10–15 cells, n = 3) (B) Representative Ca^{2+} responses of cells treated with or without the Gq inhibitor YM-254890 (1 μM). (C) Two representative traces of averaged response from Caco-2 cells loaded with FluoZin3, used to monitor changes in intracellular Zn^{2+} levels. Cells were treated with Zn^{2+} (100 μM) as in A, and no

intracellular Zn^{2+} rise is observed. Cells were then treated with Zn^{2+} (100 μM) in the presence of the ionophore pyrithione, which induced intracellular Zn^{2+} accumulation. This was not reversed by the nonpermeable Zn^{2+} chelator EDTA (100 μM), but was totally diminished by the cell permeable TPEN (40 μM). (10–15 cells, n = 3) (D) NKCC/KCC cotransporter activity was monitored in Caco-2 cells by the pH_i-sensitive BCECF fluorescent dye (1 μM) using the NH_4Cl paradigm. Addition of NH_4Cl, at the marked time, induced initial alkalization (increase of BCECF fluorescence, due to passive diffusion of NH_3 and subsequent equilibration of NH_3 and NH_4^+), followed by acidification (decrease of BCECF fluorescence, due to K^+-dependent transport using NH_4^+ as a surrogate) at a rate representing NKCC/KCC activity (see Section 4). Shown are pH_i changes in Caco-2 cells perfused with NH_4Cl following treatment with Zn^{2+} (100 μM, n = 4) or without Zn^{2+} (control, n = 4) in the presence or absence of the Gq inhibitor YM254890 (1 μM, n = 3) or the MAPK inhibitor U0126 (1 μM, n = 4). (E) Bar graph represents the normalized initial rate of K^+/Cl^- transport (initial acidification rate determined from the time a maximal signal was reached and calculated over a 70 s period, in the presence of NH_4Cl) as fold increase of the rate of acidification monitored in control cells not treated with Zn^{2+} (control). (* p 0.05 vs. control; # p 0.05 and mean ± SEM).
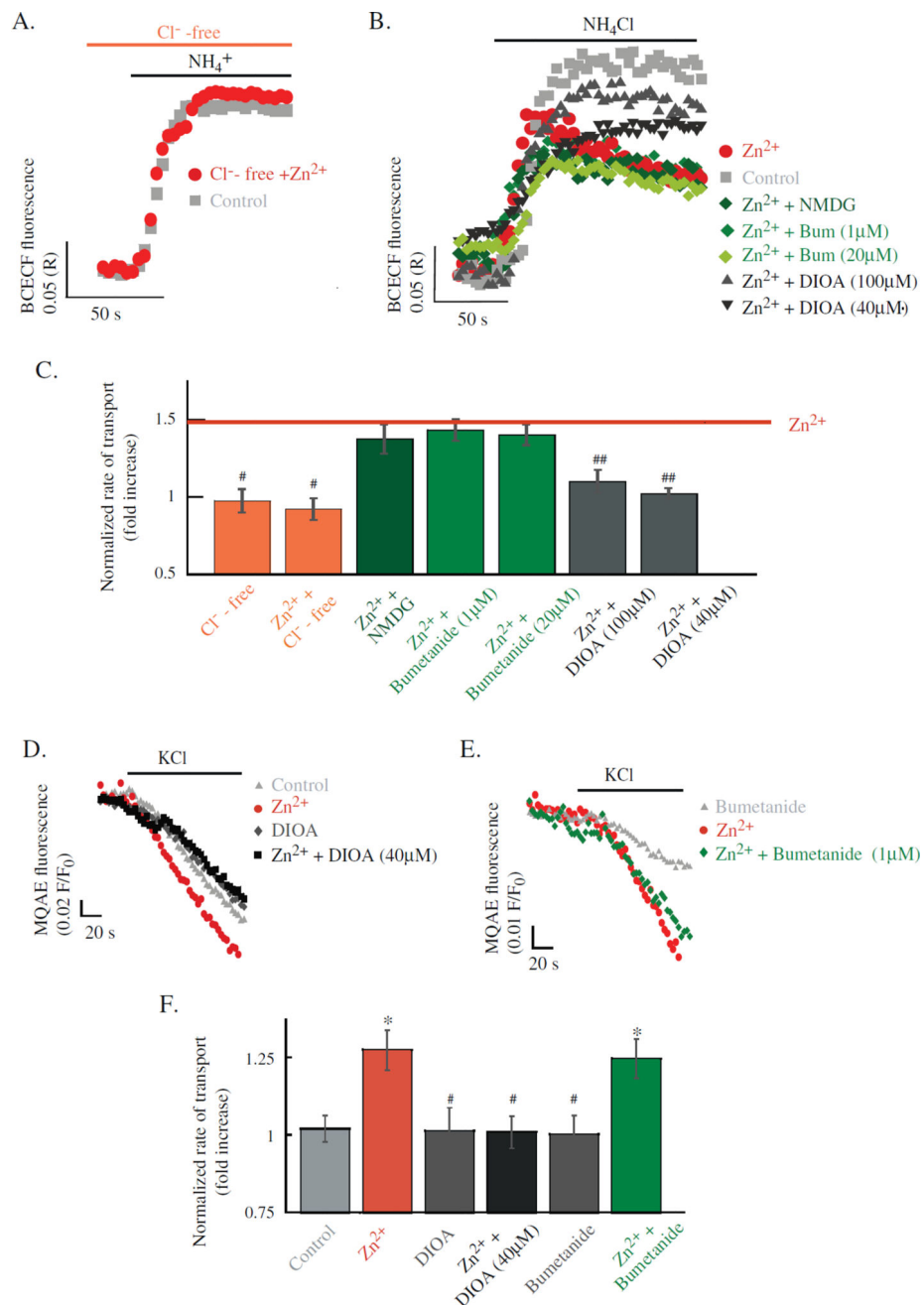
Fig 3.

Zn^{2+} upregulates Cl^- extrusion by KCC cotransporter in Caco-2 cells. (A) The ion transport paradigm, described in Fig. 2D, was performed in Caco-2 cells perfused with Cl^--free (sodium gluconate containing solution). Addition of $(NH_4)2HPO_4$ resulted in intracellular alkalinization, which was not followed by acidification. (B) The NH_4Cl paradigm, described in Fig. 2D, was performed in Caco-2 cells perfused with Na^+-free, NMDG-containing, Ringer's solution (NMDG, n = 8) or in Caco-2 cells pretreated with the NKCC inhibitor bumetanide (1 μM or 20 μM, n = 5) or the KCC inhibitor DIOA (40 or 100 μM, n = 8). (C) Bar graph represents the normalized initial rate, as measured in A–B, of K^+ transport (initial

acidification rate determined from the time a maximal signal was reached and calculated over a 70 s period, in the presence of NH_4^+) as fold increase of the rate of acidification monitored in control cells not treated with Zn^{2+} (control, line indicates the increased rates measured in Zn^{2+}-treated cells, see Fig. 2D, E). (# p 0.05 or ## p 0.01 vs. Zn^{2+} treatment; mean ± SEM) (D) Changes in intracellular Cl^- levels were monitored, by quenching of MQAE (5 mM) fluorescence, following superfusion of the cells with KCl (20 mM, as indicated). Caco-2 cells treated with KCl served as controls (n = 8), and some cells were pre-treated with Zn^{2+} (100 μM, n = 8) in the presence or absence of the KCC inhibitor DIOA (40 μM, n = 8). (E) Caco-2 cells loaded with MQAE, as in D, were treated with or without the NKCC inhibitor bumetanide (1 μM, n = 8) and Zn^{2+} (100 μM, n = 8). (H) Bar graph represents the average initial rate of Cl^- accumulation (decrease of MQAE fluorescence over a 35 s period) as fold increase of the rate monitored in control cells without Zn^{2+} pretreatment. (* p 0.05 vs. control; # p 0.05 and ## p 0.01 vs. Zn^{2+} treatment; mean ± SEM).

Fig 4.

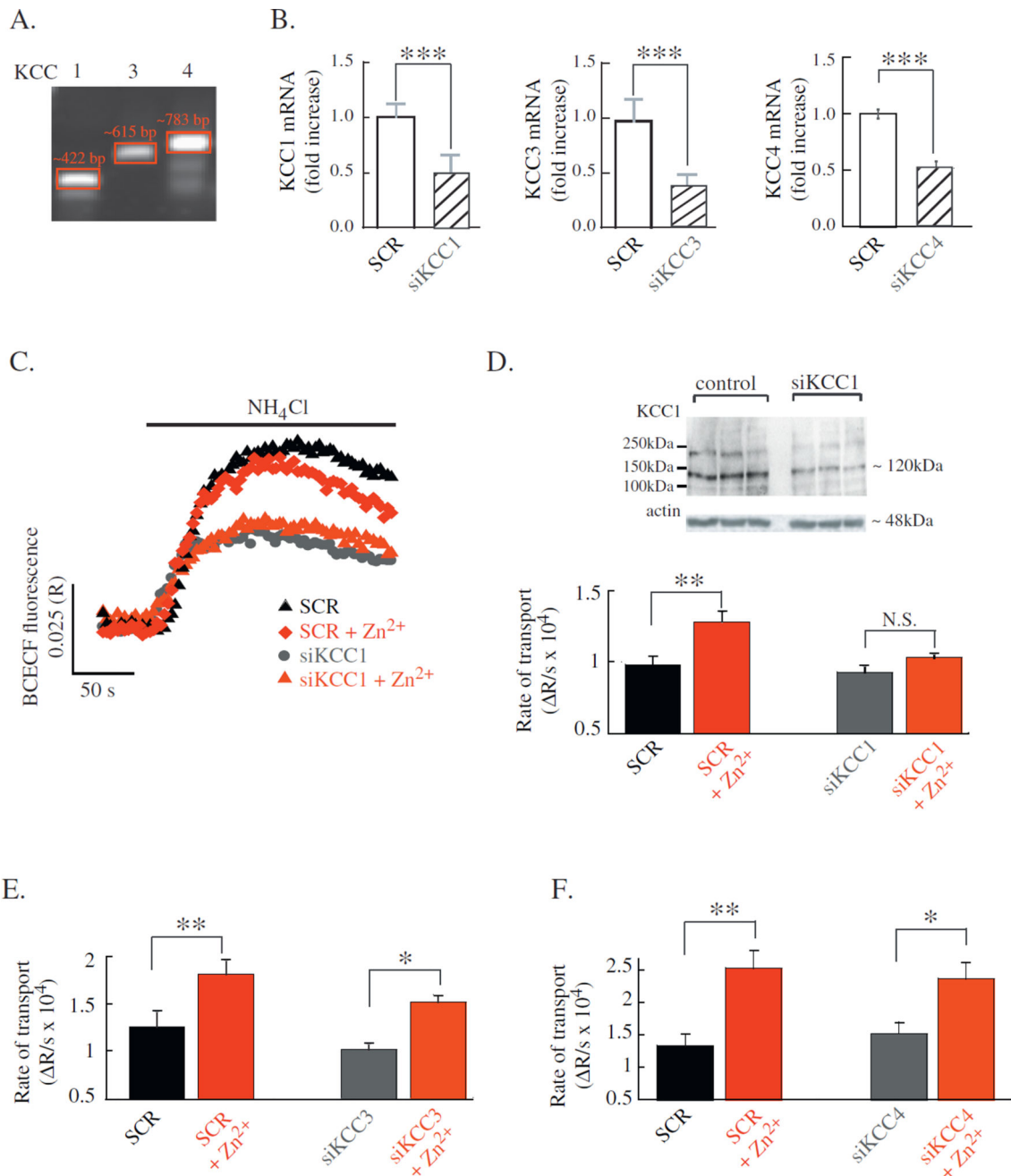Zn^{2+} upregulates Cl^- extrusion by KCC1 cotransporter in Caco-2 cells. (A) PCR analysis of Caco-2 cells using primers for the epithelial isoforms of KCC (1, 3 or 4). Note that red rectangles mark the expected size of the transcripts. (Representative of n = 3) (B) Cells were transfected with siRNA constructs: siKCC1 and siKCC3 or with a scrambled (SCR) sequences and mRNA levels were determined using quantitative PCR. (*** p   0.001 vs. SCR; mean ± SEM; n = 3) (C) Traces of BCECF fluorescence monitored as in Fig. 2D, represent K^+/Cl^- transport activity, in cells transfected with siKCC1 or scrambled (SCR) control that were treated with or without Zn^{2+} (100 µM), (n = 5 in all groups). (D) Top

panel: protein expression of cells transfected with siKCC1 monitored using western blots. (Representative of n = 3) Bottom panel: bar diagrams depict average rate of initial acidification (rate determined over a 70 s period from the maximal signal), representing KCC activity, as monitored in cells transfected with siKCC1. (E & F) Bar graphs for the ion transport rates determined using the NH_4Cl paradigm, as in C, in cells transfected with siKCC3 or siKCC4 or their relative SCR controls. (n = 5 in all groups; * p 0.05, ** p 0.01, vs. cells with same plasmid but without Zn^{2+}; mean ± SEM).
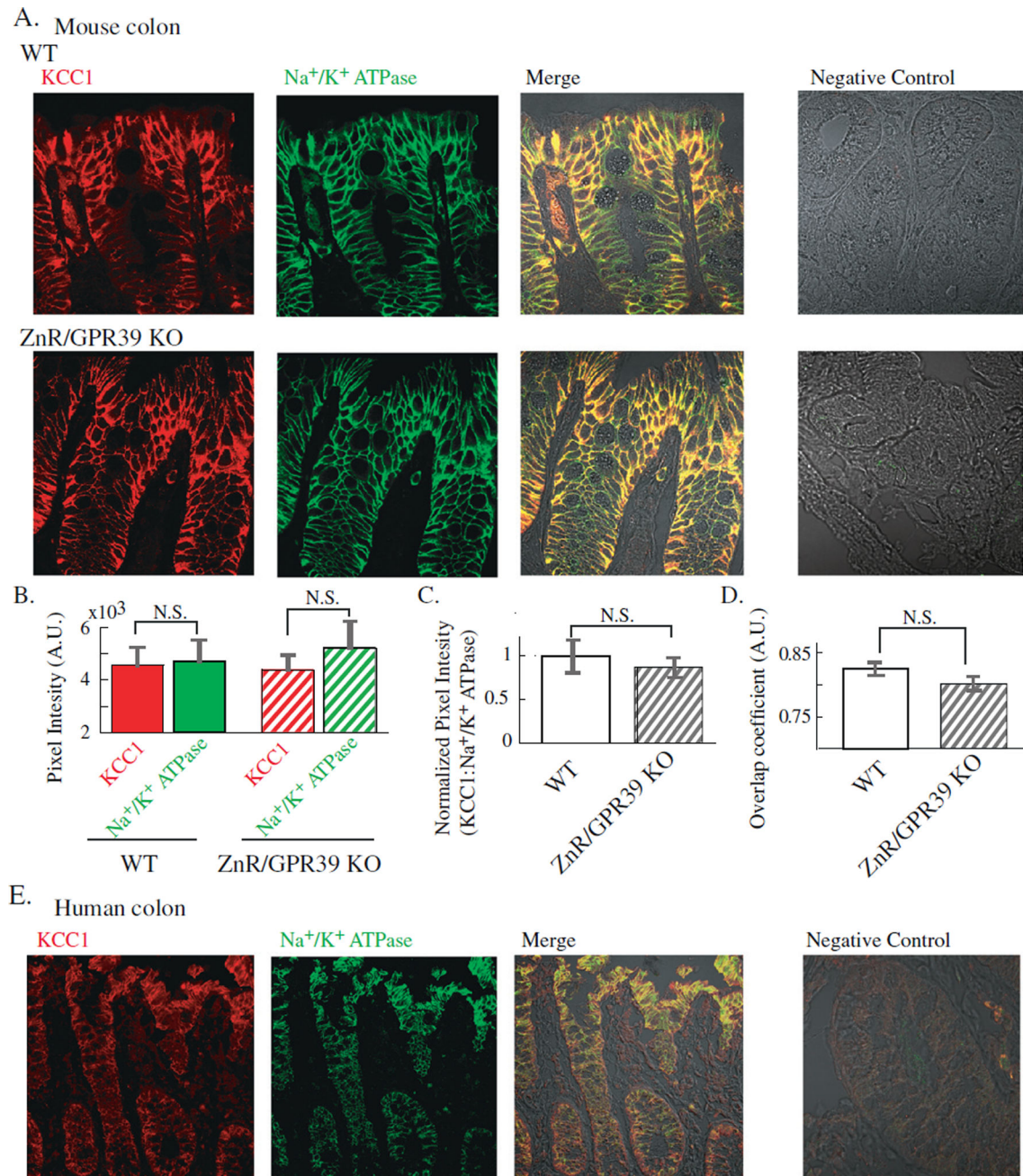
Fig 5.
KCC1 cotransporter is basolaterally expressed in mouse and human colonocytes. (A) Sections through distal colon from WT (top panels) and ZnR/GPR39 KO mice (bottom panels) were stained for KCC1 (red) or Na^+/K^+ ATPase (green), for colocalization, and images were merged. Negative controls without first antibody are shown (right panels). (B) Bar diagram represents the average intensity of the pixels of KCC1 or Na^+/K^+ ATPase in WT and ZnR/GPR39 KO mouse colon tissues (n = 3 mice for each genotype, at least 3 images were analyzed per mouse, shown mean ± SEM). (C) Normalization of KCC1 expression to that of Na^+-K^+ ATPase, as measured in B, in each image suggesting that

similar levels of KCC1 were expressed in WT and ZnR/GPR39 KO tissues. (D) "Manders" overlap coefficient of KCC1 and Na^+/K^+ ATPase expression in the colon. (n = 3 mice for each genotype, at least 3 images were analyzed per mouse, shown mean ± SEM). (E) Immunohistochemical staining of human colon tissues showing the same pattern of KCC1 (red) and Na^+/K^+ ATPase (green) expression as in mouse, see A. (n = 2 tissue sections; image shown is a representative result).
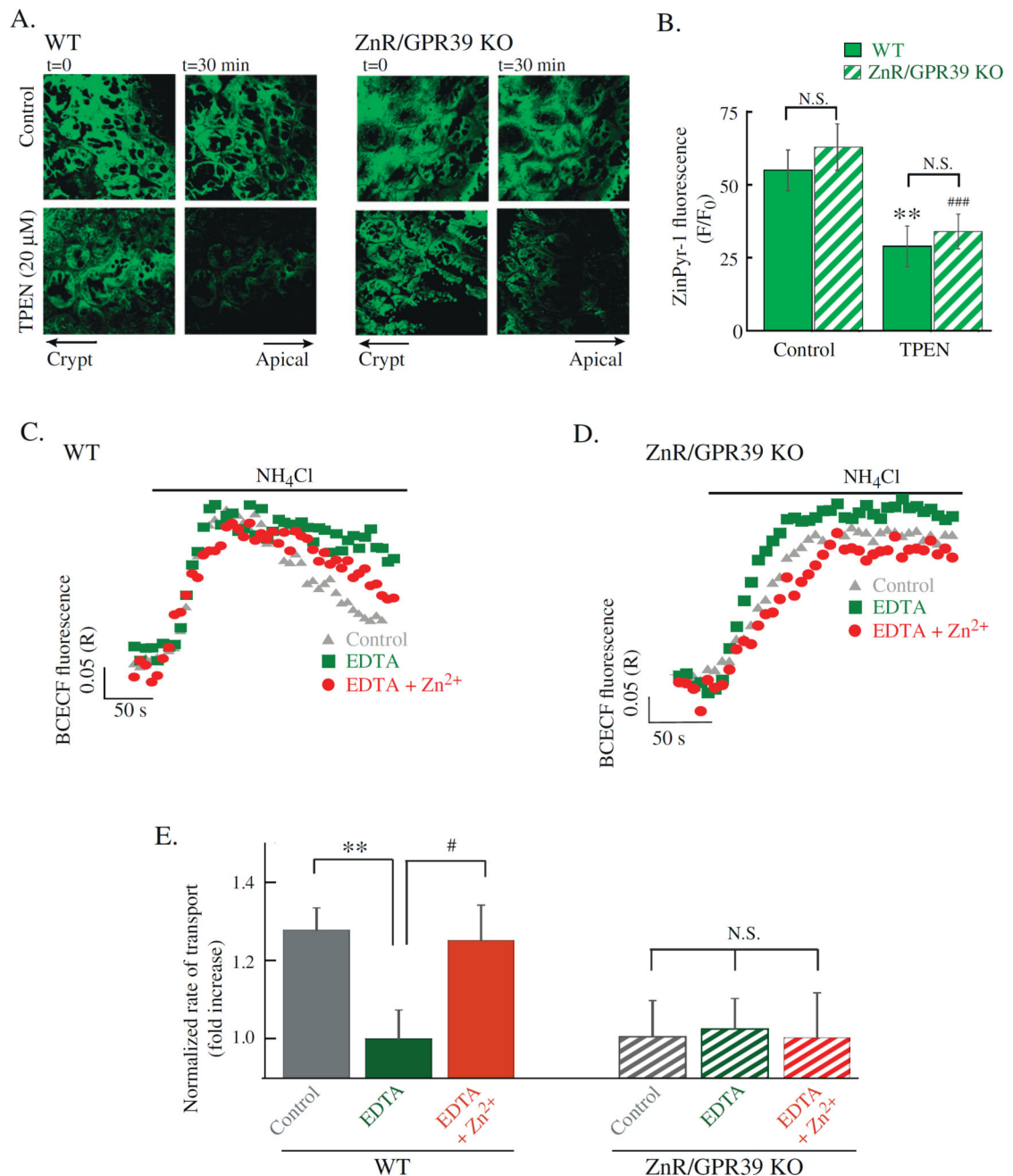
Fig 6.

Endogenous Zn^{2+} upregulates KCC cotransporter activity in colon from WT but not ZnR/GPR39 KO mice. (A) Cryostat sections of WT or ZnR/GPR39 KO mouse proximal colon tissue (30 μm) were loaded with the vesicular Zn^{2+}-sensitive fluorescent dye, Zinpyr-1 (20 μM) as was previously done [53–55], and images were acquired at the indicated times in the presence or absence of the cell permeable Zn^{2+} chelator TPEN (20 μM) at magnification ×40. (B) Averaged intensity of fluorescence in colon sections from WT and ZnR/GPR39KO mice that were treated with or without TPEN (at 30 min), as in A. A similar decrease of the signal in the presence of TPEN indicates that the Zn^{2+}-dependent fluorescent signal is

similar in WT and ZnR/GPR39 KO tissue(n= 5 for each experimental paradigm). (C) KCC transporter activity was monitored in WT colonocytes using BCECF(5 μM) loaded colon tissue. Application of NH_4Cl to the luminal side results in initial alkalinization and subsequent KCC-dependent acidification (as in Fig. 2). Tissues were washed with or without EDTA (100 μM) during preparation, to chelate endogenously released Zn^{2+}, enabling the assessment of the role of Zn^{2+}. Some tissues were treated with excess Zn^{2+} (200 μM 2 min, resulting in free-Zn^{2+} in the presence of EDTA, red). Traces of BCECF fluorescent signal are shown. (D) Colon tissue from ZnR/GPR39 KO mice were treated as in C, representative BCECF traces are shown. (E) Average initial rates of NH_4^+ influx (initial acidification rate determined from the time of maximal signal reached and calculated over a 70 s period in the presence of NH_4Cl) as monitored in (C) WT and (D) ZnR/GPR39 KO colon tissue, representing KCC activity (n = 8 for control or EDTA in WT; n = 6 for Zn^{2+} and EDTA; n = 7 for ZnR/GPR39 KO). Rates of K^+/Cl^- transport are presented as a fold-increase of basal KCC activity (WT control). (**p 0.01 compared to WT control, # p 0.05 compared to WT EDTA + Zn^{2+}; ### p 0.01 compared to ZnR/GPR39 KO control, mean ± SEM).

A.

CTx   CTx+DIOA (500 µM)
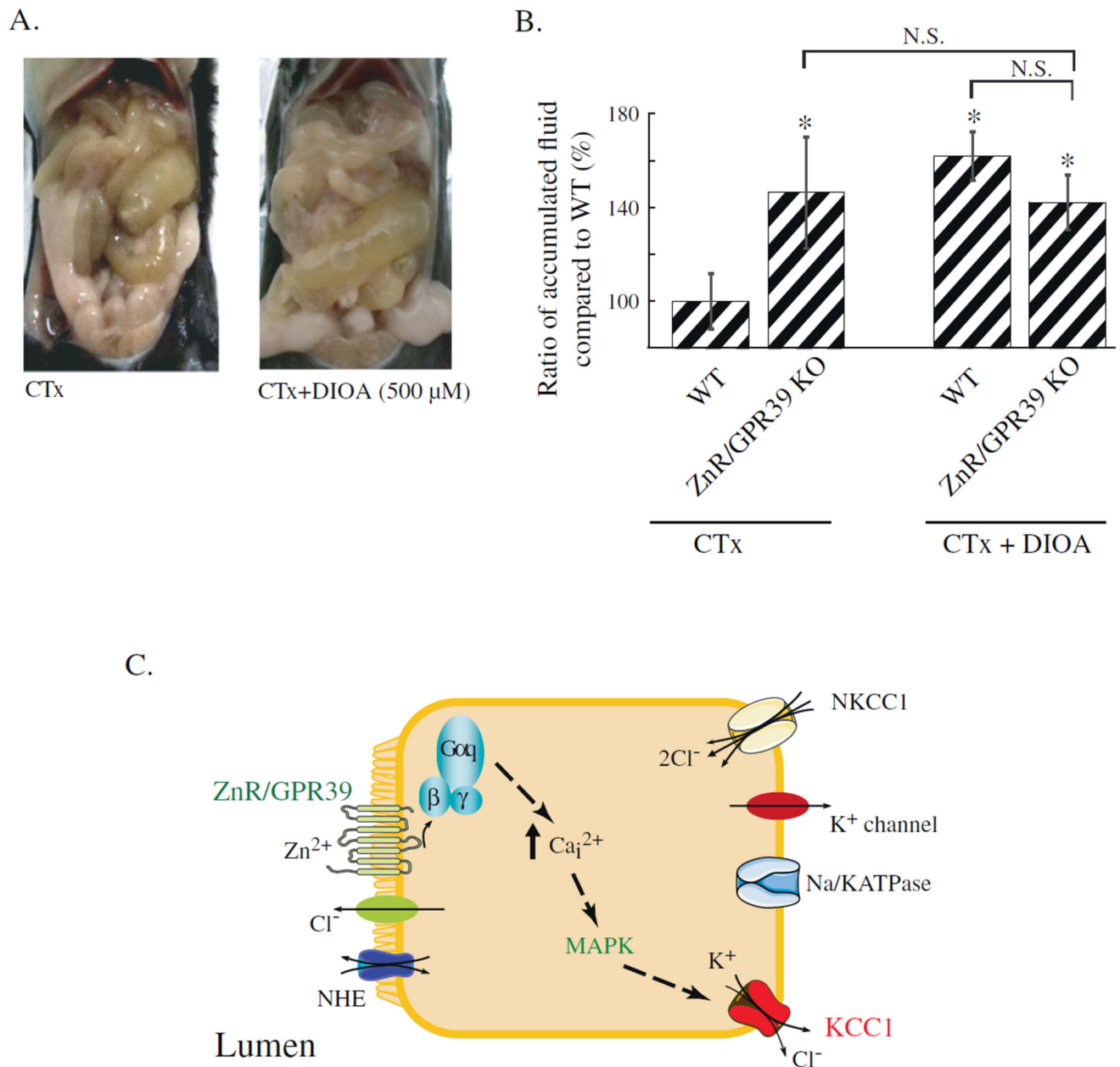
B.

C.

Fig 7.
DIOA reverses the effect of ZnR/GPR39 on cholera-toxin induced fluid secretion. (A) Mouse intestines following 6 h of gavage with cholera-toxin in the presence or absence of DIOA (500 µM). (B) Intestinal fluid secretion was measured in WT or ZnR/GPR39KO mice following 6h of cholera-toxin gavage (control, n = 3) applied with or without DIOA (500 µM, n = 6). The ratio of normalized fluid secretion content to body weight under all conditions compared to WT mice treated with CTx only is presented as percentage (fluid secretion in WT treated with CTx = 100%; see Fig. 1). The bar diagrams represent mean ± SEM.(* p ≤ 0.05 compared to WT with CTx). (C) Schematic diagram of a colonocyte illustrating ZnR/GPR39-dependent regulation of Cl⁻ absorption. Our results suggest that extracellular Zn^{2+} activates ZnR/GPR39 signaling, which triggers activation of the MAPK

pathway and leads to upregulation of K^+/Cl^- transport through the basolaterally located KCC1 cotransporter.